THE JOURNAL OF PHYSICAL CHEMISTRY A

Article

pubs.acs.org/JPCA

Prediction of Clathrate Structure Type and Guest Position by Molecular Mechanics

Everly B. Fleischer* and Kenneth C. Janda†

Department of Chemistry, University of California—Irvine, Irvine, California 92697-2025, United States

Supporting Information

ABSTRACT: The clathrate hydrates occur in various types in which the number, size, and shape of the various cages differ. Usually the clathrate type of a specific guest is predicted by the size and shape of the molecular guest. We have developed a methodology to determine the clathrate type employing molecular mechanics with the MMFF force field employing a strategy to calculate the energy of formation of the clathrate from the sum of the guest/cage energies. The clathrate type with the most negative (most stable) energy of formation would be the type predicted (we mainly focused on type I, type II, or bromine type). This strategy allows for a calculation to predict the clathrate type for any cage guest in a few minutes on a laptop computer. It proved successful in predicting the clathrate structure for 46 out of 47 guest molecules. The molecular mechanics calculations also provide a prediction of the guest position within the cage and clathrate structure. These predictions are generally consistent with the X-ray and neutron diffraction studies. By supplementing the diffraction study with molecular mechanics, we gain a more detailed insight regarding the details of the structure. We have also compared MM calculations to studies of the multiple occupancy of the cages. Finally, we present a density functional calculation that demonstrates that the inside of the clathrates cages have a relatively uniform and low electrostatic potential in comparison with the outside oxygen and hydrogen atoms. This implies that van der Waals forces will usually be dominant in the guest−cage interactions.

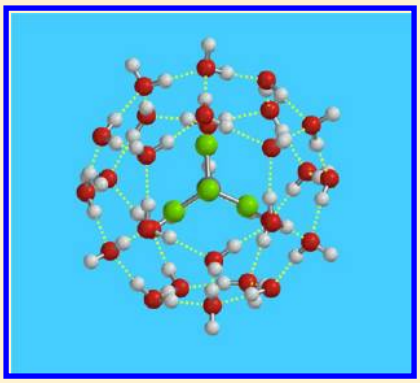

INTRODUCTION

The clathrate hydrates are both a fascinating and beautiful set of compounds as well as a chemical system that has great importance to the Earth's natural combustible gas distribution.[1] In this paper we will present a method that allows for the rapid prediction of the type of clathrate hydrate any guest will form. There is a great deal of empirical data on how the type of hydrate formed depends on the size and shape of the guest. The model presented here makes predictions regarding the clathrate type that include effects more subtle than the mean van der Waals diameter of the guest. Another important issue addressed in this paper is the specific geometry of the guest molecule inside of the cages. Despite very high quality X-ray and neutron diffraction studies on many clathrate systems, the crystal space group imposed disorder and the static and dynamic disorder within the cage makes it difficult to exactly fix the molecular guest within the cage. Our calculations that can be performed rapidly on a laptop computer are relatively simple but the insights gained are quite profound.

Methodology. We derive a straightforward algorithm that allows the energy of a clathrate cage with and without a guest to be calculated using the MMFF force field within the Spartan molecular mechanics package.[2] This paper will focus on type I, type II, and type bromine clathrate structures but the methodology we have developed can be applied to type H or any of the other types that have been or will be observed. Prior to adding the guest molecules to the calculation, we built the various cages by downloading the X-ray diffraction studies coordinates into the program Crystal Maker[3] 7.2.1. CrystalMaker produces the coordinates of the oxygen atoms and the half-hydrogen atoms that are disordered. After the desired cage is isolated, there are four half-hydrogen atoms attached to each oxygen atom. Half of these half-hydrogen atoms are eliminated to yield the correct stoichiometry. Care is taken to choose the remaining hydrogen atoms such that a proper selection of covalent and hydrogen bonds is obtained and a relatively small net dipole moment of the cage results.[4−12] In a real clathrate hydrate the location of the hydrogen atoms will fluctuate between many possible orientations. Here, we use frozen positions to calculate energies. One also has to pay attention to the number and orientation of hydrogen atoms pointing out of the cage to ensure a proper structure with a small dipole moment. The following cages were constructed: (see the Supporting Information for the coordinates of these cages) $(H_2O)_{20}$-5^{12}, $(H_2O)_{24}$-$5^{12}6^2$, $(H_2O)_{26}$-$5^{12}6^3$, $(H_2O)_{28}$-$5^{12}6^4$, $(H_20)_{36}$-$5^{12}6^8$, $(H_2O)_{20}$-$4^3S^6S^3$. Consult Figure 1 for the cages showing only the oxygen vertices and see Figure 2 showing the oxygen and hydrogen atoms as well as the hydrogen bonds of the cages. All the computations were carried out on an Apple MacBookPro with Mac OS X 10.5.8. There are quite a few

Received: November 16, 2012
Revised: April 18, 2013
Published: April 19, 2013

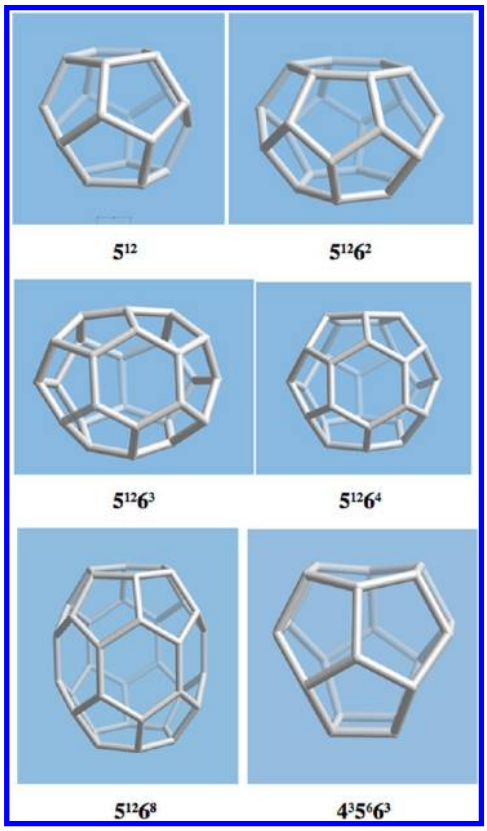

Figure 1. Clathrate cages stick model, oxygen atoms only.

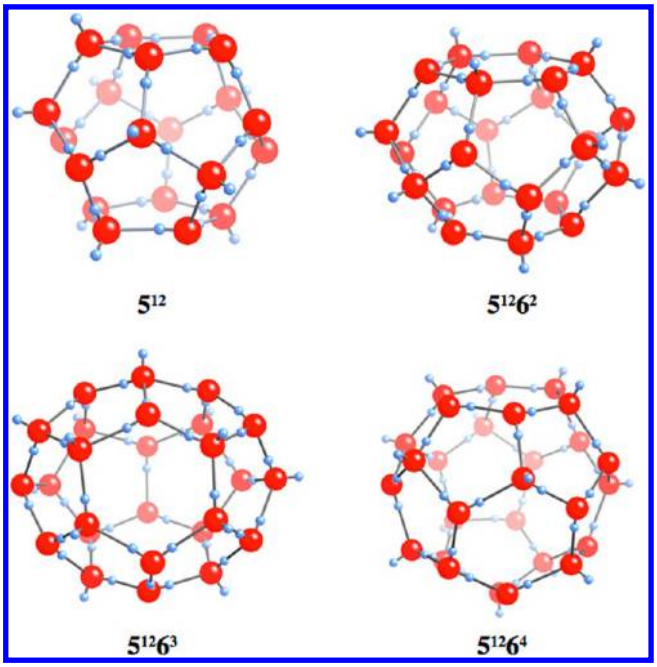

Figure 2. Principal hydrate clathrate cages with all H and O atoms.

papers in the literature employing a higher level QM and DF ab initio calculations on clathrates and several references to these papers are included here.[13−17]

Once we build a specific cage and freeze its coordinates, a guest molecule is then inserted inside of the cage and the cage−guest energy is minimized using the Spartan molecular mechanics routine. All guest atom coordinates remain flexible during this procedure. To test the robustness of this procedure, three initial guest configurations within the cage are tested in each case, and a resulting minimum is found. Usually the resulting energies of local minima are within 1 kJ/mol of the average of the three values. Upon closer inspection, these local minima only vary by slight differences due to the fact that the cage symmetries are broken by the local hydrogen-bonding structure. If one used the original half-hydrogen positions with full symmetries, these would be symmetry related minima with identical energies. For the purpose of the subsequent calculations, we use the average of the three energy values as the energy of the cage−guest pair. We then can calculate the energy of each cage empty, build any guest molecule we are interested in, and insert it inside the cage and then minimize the frozen cage with the guest inside employing molecular mechanics (MMFF in Spartan 10; see ref 18 and page S31 of the Supporting Information for the Spartan MMFF94 Compliance Statement) to obtain the frozen cage plus guest minimized energy. We then calculate the stabilization energy (E^{st}) for each cage. The stabilization energy (E^{st}) is the energy of the cage with guest (E_{cg}) minus the energy of the empty cage (E_c) plus the energy of the guest alone (E_g).

$$E^{st}{}_{nm} = E_{cg} - (E_c + E_g)$$

The subscript "nm" specifies the number of water molecules in the cage. The values obtained are given in Table S2 of the Supporting Information. In some cases discussed in more detail below, "true" higher energy local minima are found that would not be interchanged if the cages were symmetric. In these cases, the barrier for conversion to the lowest energy minima are large enough that minimization does not find the lowest minima. These energies are not used to calculate the guest−host interaction energy but are used in the analysis of X-ray data as will be described below.

The stable (guest in a cage) cages have a negative E^{st}. We then assume that the total stabilization energy for a particular type of clathrate is an additive sum of the stabilization of all the cages in the filled clathrate. It is assumed that any individual cage that has a positive E^{st} will not be filled due to the unfavorable energy. In these cases E^{st} is set to 0.0 to denote that the cage with this guest in it will not be stable as far as our criteria are concerned. See Table S2 in the Supporting Information for the actual values of these positive energies. The stabilization energy for each clathrate guest in each clathrate type is calculated as below.

$$E^{st}(\text{type I}) = ((2E^{st}{}_{20} + 6E^{st}{}_{24})/46) \times 100 \quad (1)$$

$$E^{st}(\text{type II}) = ((16E^{st}{}_{20} + 8E^{st}{}_{28})/136) \times 100 \quad (2)$$

$$E^{st}(\text{type Br}_2) = ((10E^{st}{}_{20} + 16E^{st}{}_{24} + 4E^{st}{}_{26})/172) \times 100 \quad (3)$$

Note that the stabilization energies are per 100 mol of water. This is an arbitrary number to set all the energies on the same number of waters to make the decision of which clathrate type will form with 100 mol of water. Thus, the most negative E^{st}(type X) for a particular guest will be the most stable configuration. Because the model is necessarily overly simple, we employ a criterion for selection of a clathrate type to have the E^{st} at least 15 kJ/mol more stable than the next type to make a "firm" assignment.

dx.doi.org/10.1021/jp311351j | J. Phys. Chem. A 2013, 117, 4001−4010

RESULTS AND DISCUSSION

A. Clathrate Crystal Stability. Table 1 presents the calculated stabilization energy for type I and type II structures,

Table 1. Clathrate Type Stabilities and Type Predictions for Type I and Type II Clathrates (Energies in kJ/100 mol of H_2O)

guest	E^{st}(type I)	E^{st}(type II)	prediction	experiment
CO_2	−272	−198	I	I
propane	−28	−263	II	II
Xe	−185	−133	I	I
Kr	−177	−167	I/II	I/II
Ar	−156	−161	I/II	I/II
I_2	0	−95	II	II (in subst)
Br_2	−78	−122	II/Br_2	II/Br_2(−112)
Cl_2	−223	−99	I	I
F_2	−100	−65	I	unknown
CH_4	−274	−211	I	I
H_2S	−331	−146	I	I
C_2H_6	−299	−119	I	I
cyclopropane	−273	−155	I	I
CH_2ClF	−242	−174	I	I
$CBrF_3$	0	−140	II	II
CH_3Br	−181	−170	I	I
CH_3Cl	−263	−164	I	I
CH_2Cl_2	−9	−184	II	II
$(CH_2)_3O$	−234	−226	I/II	I/II
THF	0	−226	II	II
i-C_4H_{10}	0	−200	II	II
n-C_4H_{10}	0	−168	II	II
N_2	−171	−111	I	I
BrCl	−180	−127	I	I
PH_3	−236	−201	I	I
SF_6	−305	−347	II	II
CH_3F	−506	−362	I	I
CH_2F_2	−413	−375	I	I
CF_4	−256	−89	I	I
CH_3CH_2F	−292	−173	I	I
CH_3-O-CH_3	−167	−182	II/Br_2	II/Br_2(−196)
CH_3COCH_3	0	−250	II	II
CH_3I	0	−179	II	II
benzene	0	−177	II	II
O_2	−149	−108	I	I
N_2O [a]	−821	−620	I	I
SO_2	−401	−388	I	I
CH_3CHCH_2	−103	−152	II	II
cyclopentane	0	−222	II	II
$(CH_3)CF$	0	−223	II	II
C_2H_5Cl	−98	−193	II	II
CH_3CHCl_2	0	−196	II	II
$CHClF_2$	−192	−172	I	I
CCl_2F_2	0	−146	II	II
CCl_3F	0	−138	II	II
CH_3CClF_2	−3	−195	II	II
$CBrF_3$	−46	−141	II	II

the predicted stable structure and the observed structures for the 47 guest molecules we examined. Although our model is quite rudimentary, the results are remarkably predictive. In each case for which the stabilization energy of two types is different by more than 15 kJ/mol, our model predicts the correct result. There are five cases that have the two energies of two types within 15 kJ of each other. Three of those, the Br_2, $(CH_2)_3O$, and CH_3-O-CH_3, exist in each of the two types predicted. For the other two, Kr and Ar, the prediction is correct for Ar, but incorrect for Kr. The remarkable success of the results presented in Table 1 gives us confidence that the algorithm presented here will predict the crystal type for most guest molecules that could form a hydrate. Even though we restricted our calculations to the type I, type II, and type Br_2, the method should also work for predictions on type H or any other type of clathrate.

As discussed above, in 90% of the test cases the prediction is unambiguous. Trimethylene oxide can be found in both type I and type II crystals. In this respect it is interesting to note that the molecule is too large to fit into the 5^{12} cages and is more than twice as stable in the $5^{12}6^4$ cage than in the $5^{12}6^2$ cage. This is balanced out by the larger number of $5^{12}6^2$ cages in the type I structure than $5^{12}6^4$ cages in the type II. Dimethyl ether is particularly stable in the $5^{12}6^3$ cage, resulting in the observation of the Br_2 type crystal structure.

The series Ar, Kr, and Xe is also instructive. Xenon is most stable in the $5^{12}6^2$ cage, most prevalent in the type I structure. The type-I stability is further enhanced by its stability in the 5^{12} cage. For Kr, the results are similar, with somewhat enhanced stability in the 5^{12} cage. This moves the stability toward type-II enough that our model is ambiguous. The trend continues for Ar, and although the model is still ambiguous, the absolute prediction of clathrate type is now correct. It is also interesting that the model predicted here correctly predicts the relative stability of Xenon type-I > Kr type-II > Ar type-II. Similarly, Cl_2 hydrate is correctly predicted to be more stable than Br_2 hydrate and the I_2 hydrate, which has yet to be observed without a helper molecule.

It is quite interesting that the calculation of relative energies results in such excellent prediction of the clathrate type without the use of the Free Energy of formation or any reference correction for entropies. In most cases, the energy difference between the two crystal types is quite large, so the results are unambiguous. Schofield and Jordan[16] calculated the effects of temperature on both enthalpy and entropy for the three Br_2 hydrate crystal types and found that the cage energy was the most important criterion. For a single guest type, temperature effects evidently cancel out enough that they can be neglected.

A rigorous calculation of relative stability would require evaluation of the chemical potential and the relative vapor pressure as a function of temperature. Such calculations are usually performed using the van der Waals−Platteeuw[20] method. In most cases, data at a given temperature are used to estimate a 1-D cage potential that can then be used to extrapolate the data to other potentials. Only for a very important system such as methane hydrate[13,17] have completely ab initio attempts to calculate stability been attempted. For many of the guest molecules examined here, a 1-D potential would be quite unphysical, so that ab initio methods would necessarily entail a detailed attempt to account for the angular dependence of the potential. Schofield and Jordan[16] calculated the relative stability of Br_2 hydrate crystals from first principles and obtained the correct result. However, the difficulty of that study highlights the utility of the much less rigorous method presented here.

Although it does not affect the predictive value of our model, we note here that the cage energies, E_c, calculated using the MMFF potential are also in reasonable agreement with the accepted value of hydrogen bond energies. If E_c is divided by

dx.doi.org/10.1021/jp311351j | J. Phys. Chem. A 2013, 117, 4001−4010

the number of hydrogen bonds for each cage, one gets an average hydrogen bond energy for each cage. This calculation leads to 19.9 kJ/mol for the 5^{12} cage (30 hydrogen bonds), 22.6 kJ/mol for the $5^{12}6^2$ cage (36 hydrogen bonds), and 23.2 kJ/mol for the $5^{12}6^4$ cage (42 hydrogen bonds), which are close to the usual hydrogen bond energy in ice of 21 kJ/mol. This is probably not too surprising because the MMFF potentials are used extensively for aqueous simulations and optimized accordingly.

B. Guest Position and Orientation in Clathrate Cages. We will now test the MMFF/molecular mechanics prediction of guest orientation within the cages by comparing to X-ray and neutron diffraction studies. There are many excellent X-ray and neutron diffractions studies of clathrate compounds employing single crystal and powder diffraction methods. These diffraction studies define the oxygen atoms of the clathrate cages with very high accuracy; the water hydrogens are disordered in the clathrates and thus there are four half-hydrogens on each water oxygen in the X-ray structures, as discussed previously. The average positions of these half-hydrogens are also well-defined. On the other hand, the guest positions and orientations in the cages are not well-defined because there are both crystallographic disorder and positional disorder of the guests in the clathrate crystals. Also there will be dynamic disorder due to guest motion. The space group required disorder of a guest in these cages might be 8-, 12-, or 24-fold depending on the clathrate type and cage. The authors of the crystallographic studies have done an admirable job of untangling this complicated geometrical problem. We show that the molecular mechanics in our studies allows for a usefully accurate positioning of the guest within each cage. This will be helpful to the diffraction studies as well as providing insight into the details of cage structure for which unambiguous results have yet to be obtained. One could apply the crystal symmetry to the calculated guest position and then generate a model of what the X-ray or neutron diffractions studies might see.

The methane clathrate forms a type I system with methane in both the small 5^{12} and the large $5^{12}6^2$ cages. The X-ray study[19] has the methane in the center of the small 5^{12} cage with the hydrogens 12-fold disordered and each one pointing toward the middle of a pentagonal face. In contrast to the diffraction studies, the MM method makes a simple and unambiguous prediction of the guest position within the cage. In this case, this allows the hydrogen atom orientations to be easily predicted. The MM predicts that the methane is located in the center of the cage, within 0.05 Å, as shown in Figure 3 with three of the hydrogen atoms of the methane pointing to a pentagonal face and one at a water oxygen atom of the cage.

The diffraction results for the $5^{12}6^2$ cages are more ambiguous. They[19] suggest that in the $5^{12}6^2$ cages the methane is fully disordered around the center of the cage without a clear indication exactly where it is positioned. Our calculations show that the methane is always centered between the two hexagonal planes (2.97 Å from each hexagonal plane) whereas it is off center by 0.48 Å from the plane that is perpendicular to the hexagonal face and through the center, as shown in Figure 4. Thus we can show with some confidence where the lowest energy configuration for methane or other guests are positioned in a cage. We can generate the various equivalent positions in the cage that the methane molecules can take up with equal energy. In this particular case there are 12 such positions. The carbon of the methane is always in the plane halfway between the two hexagonal planes of the cage. The MM calculations are

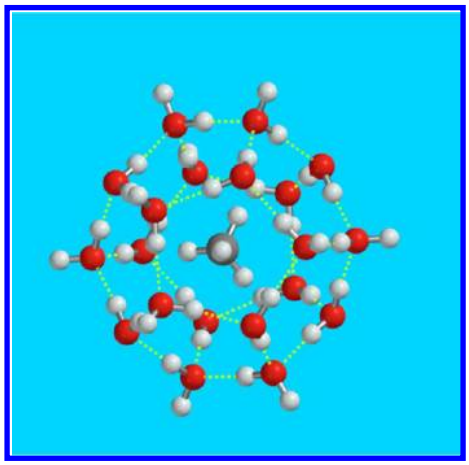

Figure 3. 5^{12} methane.

Figure 4. $5^{12}6^2$ minimized methane, side view.

completely consistent with the experimental data but also can give more subtle information than the X-ray studies. It is of interest that the higher-level quantum calculations (see refs 13b and 13c) on the methane clathrates show similar guest geometries and relative ordering of the type I and type II stabilities. These higher-level quantum calculations have the ability to produce a much more detailed description of the properties of the methane clathrate than our molecular mechanics calculations.

Reference 19 also discusses the type I acetylene clathrate. In the 5^{12} cage we find that the acetylene hydrogens point toward the centers of two opposing pentagonal faces with a slightly positive stabilization energy (7 kJ/mol). This is consistent with the low occupancy found in the small cage. In the larger $5^{12}6^2$ cage two distinct minima are found and are shown in Figures 5 and 6. For the lowest energy minimum, Figure 5, the acetylene is parallel to the hexagonal faces with 12 equivalent positions (rotated from the one in the figure by 30° increments) and an energy of −825 kJ/mol. For the second minimum, Figure 6, the acetylene is perpendicular to the hexagonal faces with the acetylene hydrogens pointing to the middle of those faces with an energy of −820 kJ/mol. The X-ray analysis is interpreted in terms of a "torus that winds along the equatorial plane" that is fit to a model that indeed is quite consistent with our calculation. Even very accurate diffraction data for acetylene hydrate may not be able to test the existence of the second perpendicular configuration because of the 12 to 1 symmetry ratio of the lower energy to the second minimum.

For the case of propane hydrate the MM method presented here adds significant insight to the diffraction analysis. Drawing

dx.doi.org/10.1021/jp311351j | J. Phys. Chem. A 2013, 117, 4001−4010

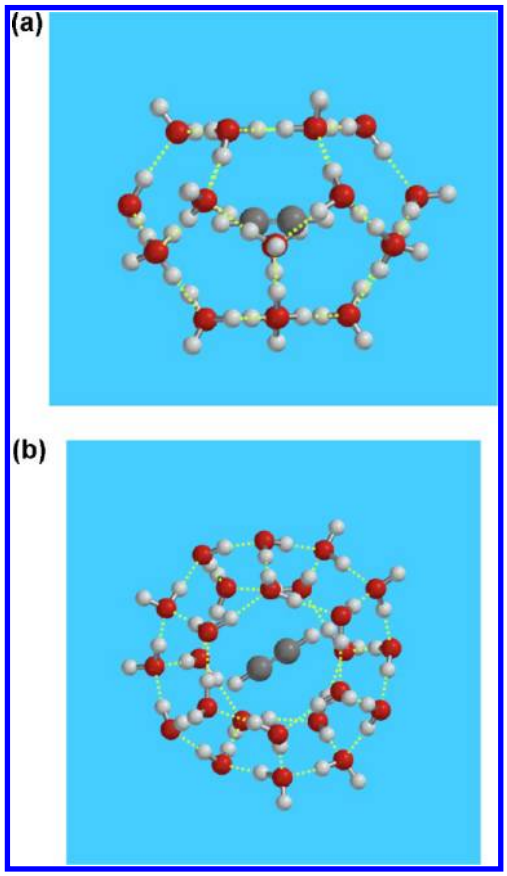

Figure 5. (a) Lowest energy C_2H_2 $5^{12}6^2$, side view. (b) Lowest energy C_2H_2 $5^{12}6^2$, top view.

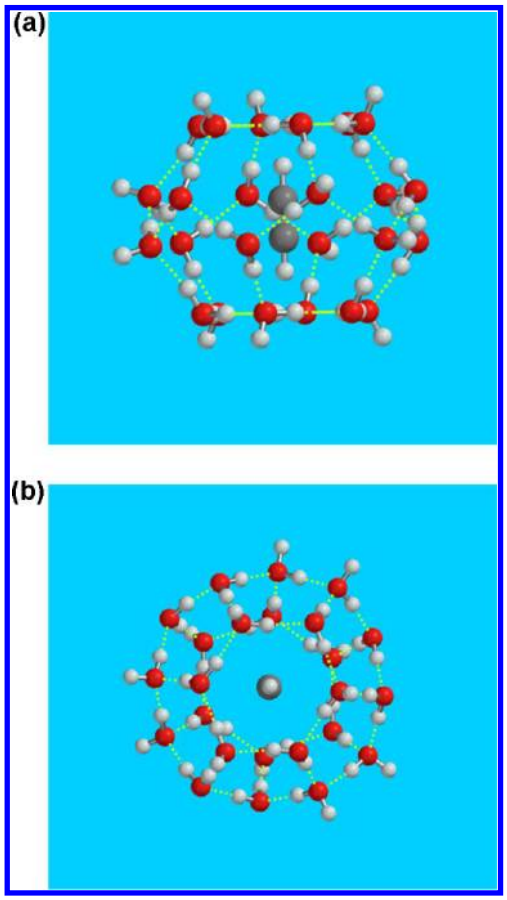

Figure 6. (a) Second minimum of C_2H_2 $5^{12}6^2$, side view. (b) Second minimum of C_2H_2 $5^{12}6^2$, top view.

Figure 7. $5^{12}6^4$ cage with propane in it.

conclusions from the X-ray structure for propane hydrate[19] is extremely difficult due to the low symmetry and flexibility of the propane and a minimum of 12-fold symmetry disorder. The author's main conclusion[19] is that the propane is not centered in the $5^{12}6^4$ cages. We tested nine crystallographically equivalent configurations, one shown in Figure 7, of the propane in the $5^{12}6^4$ cage. The average E_{cg} was 1021.1 kJ/mol with a standard deviation of 0.2 kJ/mol. These differences are due to the nonidealized oxygen atom positions taken from the X-ray studies as well as the nonsymmetrical external hydrogens and hydrogen-bonding scheme in the isolated cages.

The CCl_4−Xe double clathrate presents a very interesting example of how the MM method confirms and adds detail to the insight gained from diffraction results. The neutron diffraction study[21a] demonstrates that the Xe is in the center of the smaller 5^{12} cage and the CCl_4 is disordered in the $5^{12}6^4$ larger cage. A sophisticated model in the neutron study for the CCl_4 was employed by invoking three positions, one with about twice the occupancy of the other two and for which the proportion of the orientations were dependent on temperature. The C of the CCl_4 is centered in the large cage. Molecular mechanics calculations show that there are three nearly equal minima for the CCl_4 that are consistent with the experimental results. The most stable minimum, illustrated in Figure 8a, has each chlorine atom pointing toward a hexagonal face of the cage and a molecular mechanics energy of −996 kJ/mol, whereas the second and third minima have energies of −991 and −988 kJ/mol.

The second minimum, Figure 8b, has one chlorine pointing toward the center of one hexagonal face and the other three chlorines pointing toward three pentagonal faces. The third minimum has an orientation similar to that of the second but pointing toward different pentagonal and hexagonal faces. Thus, in this case it is demonstrated that we find the three minima with the same orientations as the diffraction study and the correct prediction of the most stable orientation and the less stable orientations.

We next discuss the structures of and trimethylene oxide (TMO) from the point of view of the diffraction studies[21−26] compared to the molecular mechanics calculations. The TMO clathrate forms a type I clathrate with the empty small cages and the TMO in the larger $5^{12}6^2$ cages. Figure 9, reproduced

dx.doi.org/10.1021/jp311351j | J. Phys. Chem. A 2013, 117, 4001−4010

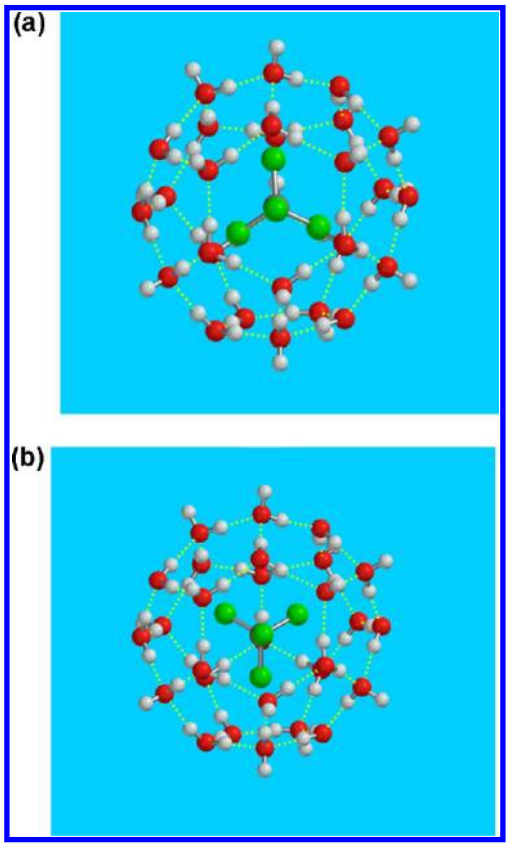

Figure 8. $5^{12}6^4$ cage with CCl_4. In (a) the Cls all point toward hexagons whereas in (b) one Cl points toward a hexagonal and three toward pentagonal faces. (a) is the minimum energy and the (b) is the second minimum.

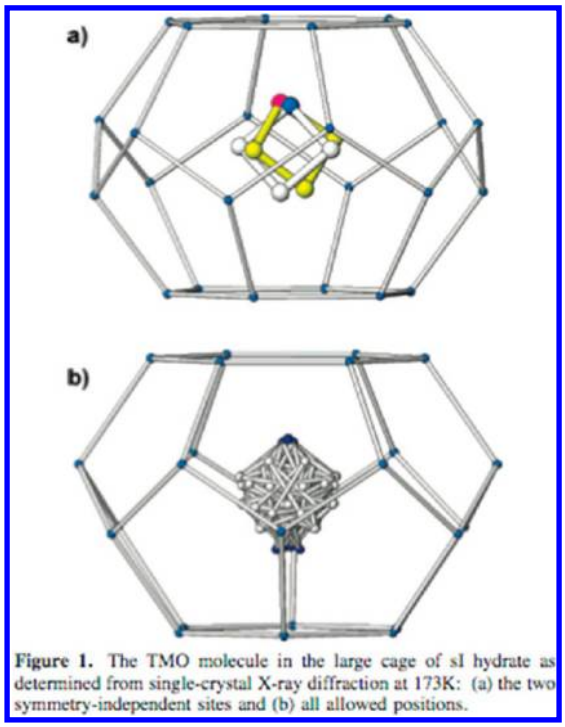

Figure 9. Figure 1 from ref 26.

from ref 26 Figure 1, shows that the TMO has two independent orientations and is disordered by 8 crystal symmetry imposed orientations.[26] The MM calculations yielded three minima for the TMO in the $5^{12}6^2$ cages, with energies of −807, −801, and −797 kJ/mol. These are shown in Figure 10−12, respectively.

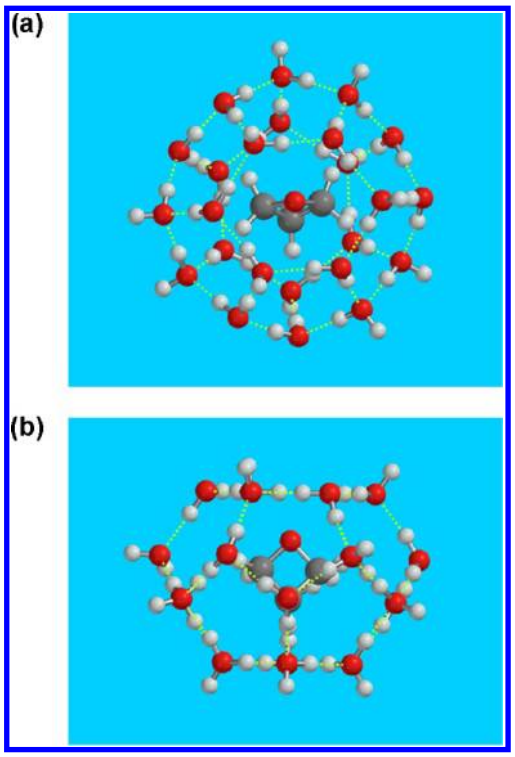

Figure 10. (a) Top view, most stable orientation of $5^{12}6^2$ TMO. (b) Side view, most stable orientation of $5^{12}6^2$ TMO.

The angle between the perpendicular to the hexagonal face and the C to O vector in the TMO is 15° for the most stable (Figure 10), 30° for the second minimum (Figure 11), and 75° for the third minimum (Figure 12). This is consistent with another paper on TMO clathrates by Rondinone[24] where they find that in the type I TMO clathrate the angle of the TMO C to O vector changes with temperature with the vector at 12° at 11 K and at 150 K is at 22°, whereas at 220 K it is 75°.

In contrast to the type I TMO clathrate, the X-ray structure of the type II TMO clathrate shows that there is no major change in orientation (other minima) of the TMO in the larger $5^{12}6^4$ cage as a function of temperature. When TMO was minimized in this cage, it had an energy of −985 kJ/mol, Figure 13, with no other higher energy minima that could be found. The equivalent orientations always have the TMO O atom aligned to the O of a H_2O looking down a hexagonal face. In the actual structure the TMO has many equivalent symmetry related orientations. These calculated orientations will be an aid in unraveling the X-ray disorder and in determining the guest orientation and structure in clathrate systems.

The CO_2 clathrate has been studied by various authors.[25,27] The X-ray study by Udachin et al.[25] is an unusually well done and accurate structure. Figure 14 reproduces Figures 1 and 2 from ref 25 and illustrates the orientations of the CO_2 in both the small and large cages of the type I structure. In the large cage they found two 8-fold orientations of the CO_2: the first eight have a 14.4° angle from the plane parallel to the hexagonal faces and bisecting the cage; the other eight have an angle of 6.5°. In a later paper[27] by the same group, a single angle of 8° is also found to be consistent with their data.

dx.doi.org/10.1021/jp311351j | J. Phys. Chem. A 2013, 117, 4001−4010

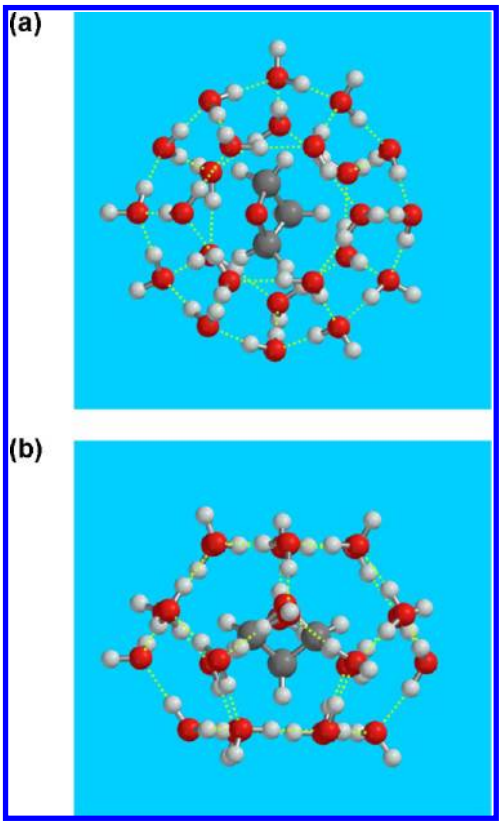

Figure 11. (a) Top view of second minimum orientation of $5^{12}6^2$ TMO. (b) Side view of second minimum orientation of $5^{12}6^2$ TMO.

Figure 12. Side view of 3rd minimum orientation of $5^{12}6^2$ TMO.

Molecular mechanics calculations are consistent with the above results with the subtlety that the C of the CO_2 is calculated to be on the bisecting plane but 0.2 Å off center and the tilt of the CO_2 with respect to the plane is 5°, roughly consistent with ref 27. As in the acetylene case, MM calculations predict a minimum shown in Figure 15 and a second minima, 5 kJ/mol less stable, shown in Figure 16, with the axis of the CO_2 going through the center of the hexagonal faces.

In every case that has been examined, the MM calculations are consistent with the diffraction data in the literature and offer an interesting perspective for interpreting the data. In the future, we suggest that combining MM calculations with the diffraction analysis will yield additional subtle information regarding the guest positions in the cages.

Figure 13. TMO in $5^{12}6^4$ cage.

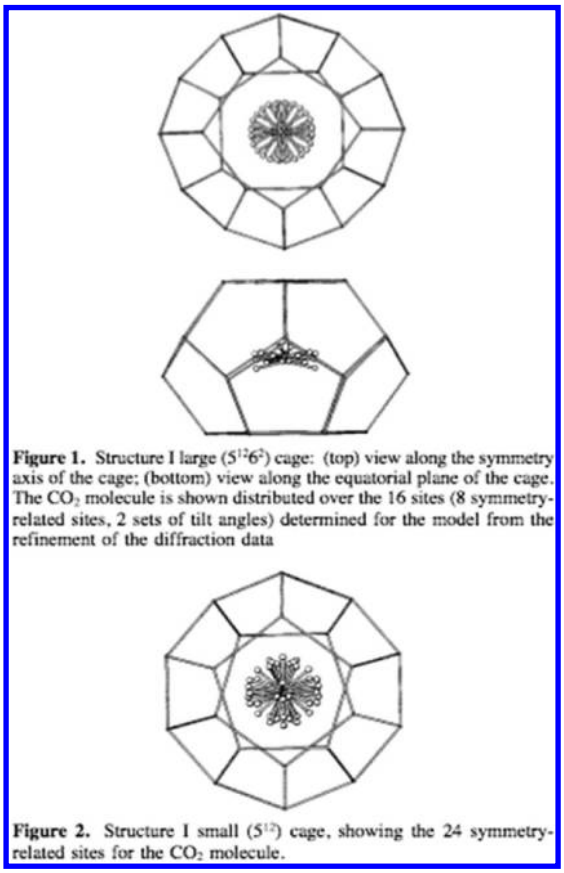

Figure 1. Structure I large ($5^{12}6^2$) cage: (top) view along the symmetry axis of the cage; (bottom) view along the equatorial plane of the cage. The CO_2 molecule is shown distributed over the 16 sites (8 symmetry-related sites, 2 sets of tilt angles) determined for the model from the refinement of the diffraction data

Figure 2. Structure I small (5^{12}) cage, showing the 24 symmetry-related sites for the CO_2 molecule.

Figure 14. Figures 1 and 2 from ref 25.

Multiple Occupancy of Cages. There are a number of both experimental and theoretical studies of multiple occupancy of the various cages in the hydrate clathrates.[28−38] For guests other than hydrogen, MM also should be useful for gaining insight into this issue. We have tested this hypothesis for the case of CO_2, Ar, and CH_4. We calculated the stability of multiple occupancy in the various cages by placing n guest molecules in the cage and minimizing the system. The procedure employed in this study was to add a guest to a cage and minimize its energy and keep adding the next guest until the system has a positive stabilization energy and thus is no longer stable. This procedure gives both the energy of the

dx.doi.org/10.1021/jp311351j | J. Phys. Chem. A 2013, 117, 4001−4010

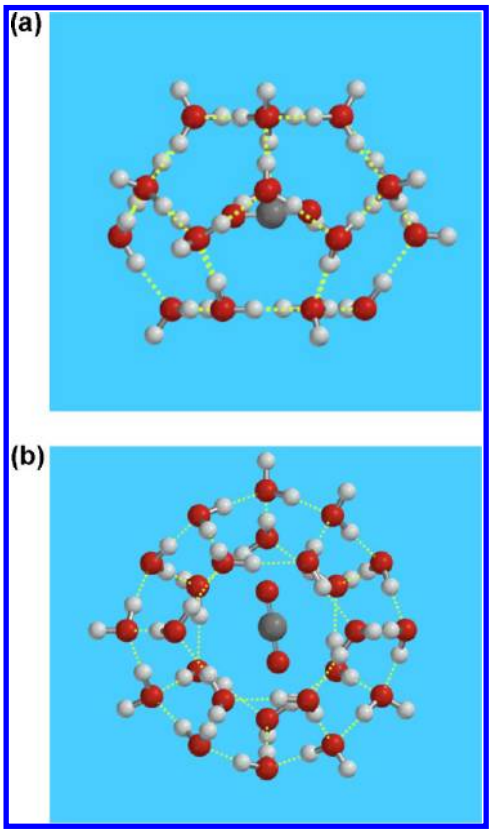

Figure 15. (a) $5^{12}6^2$ CO_2 side view. (b) $5^{12}6^2$ CO_2 top view.

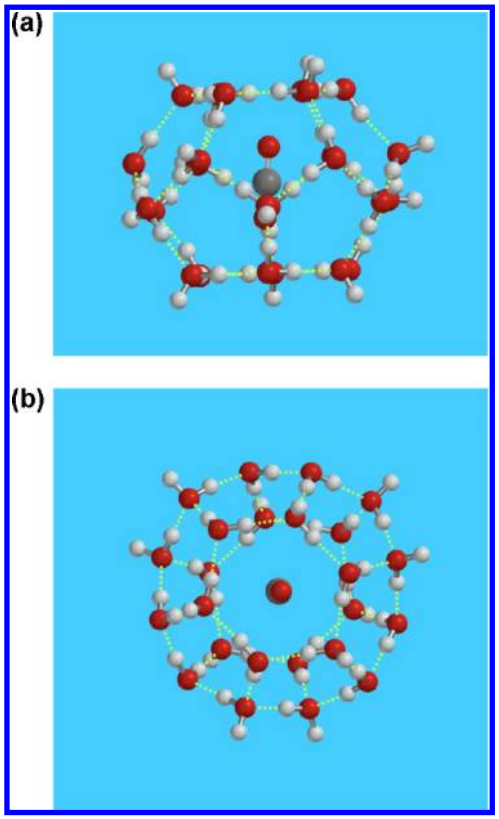

Figure 16. (a) Side view $5^{12}6^2$ CO_2, second minimum. (b) Top view $5^{12}6^2$ CO_2, second minimum.

N-guest system and the configuration of the guests within the cage. Table 2 shows the maximum occupancy that yields a

Table 2. Multiple Occupancies of CO_2, Ar, and CH_4 Guest in Various Cages

cage	CO_2	Ar	CH_4
5^{12}	CO_2-1 (1)	Ar-1 (1)	CH_4-1 (1)
$5^{12}6^2$	CO_2-1 (1)	Ar-2 (1)	CH_4-1 (1)
$5^{12}6^4$	CO_2-2 (1)	Ar-3 (2)	CH_4-3 (na)
$5^{12}6^8$	CO_2-4 (na)	Ar-6 (5)	CH_4-5 (na)

negative energy for each cage. The numbers after the dash in Table 2 are the maximum occupancy resulting from the MM calculations and the numbers in parentheses are the experimental numbers. The results in Table 2 are quite consistent with experimental data in the literature. At the very least, calculations such as those performed here can illustrate when an assumption used to interpret data is unlikely to be correct. For instance, in a theory paper[34] 6 and 7 CO_2 molecules are assumed to fit into the $5^{12}6^8$ cage. These calculations show that with more than 5 CO_2's the cage already yields a positive E^{st}. If one calculates the van der Waals nonbonding distances in the assumed 6 and 7 CO_2 cage structures of ref 34, one finds that the O---O and the O---H nonbonding distances have van der Waals spheres overlapping by at least 0.2 Å, for 7 (O---O) and 11 (H---O) for the 6 CO_2 case, and 16 and 15 for the 7 CO_2 case. The MM calculations yield $N = 3$ as the most stable structure whereas $N = 4$ is also stable. In these two cases there are no van der Waals interpenetrations. We conclude that occupancy of the $5^{12}6^8$ cage by more than 5 CO_2 molecules will be very rare. Of course, in the case of experiments conducted at very high pressure, occupancies for which the MM model yields a positive energy will be possible. A more sophisticated model would be necessary to understand cage occupancy as a function of pressure, and more experimental data are needed at high pressure to compare with our results.

Electrostatic Potential Inside the Cages. There have been a considerable number of higher level quantum mechanical calculations on clathrate systems.[13−18] Although the calculations with molecular mechanics are less sophisticated than ab initio or density functional methods, we have shown that they are useful to calculate relative energies and positions of the guests in the clathrates and clathrate type. On the other hand, the higher level calculations can give insight that is not available from the MM calculations. As we were comparing our results to more sophisticated calculations, we discovered a particular insight that we have not seen previously discussed in the literature. Using the Spartan software, we ran a density functional calculation with the EDF2/6-31G* functional and plotted the electrostatic potential surface for the $(H_2O)_{24}$ $5^{12}6^2$ cage, shown in Figure 17. Though semilocal density functionals have well-known deficiencies for long-range dispersion interactions, the electrostatics is generally accurate. The surface color is red for negative electrostatic potential, blue for positive electrostatic potential, and light green or yellow for lower or more neutral electrostatic potential. The magnitudes of the surface electrostatic potential as calculated in this case are for the deepest red, −224 kJ/mol, and for deepest blue, +268 kJ/mol. Inside the cage the pale green portion of the potential ranges from −50 to +50 kJ/mol and the pale yellow ranges from −50 to −80 kJ/mol. The lone H atoms sticking out of the

dx.doi.org/10.1021/jp311351j | J. Phys. Chem. A 2013, 117, 4001−4010

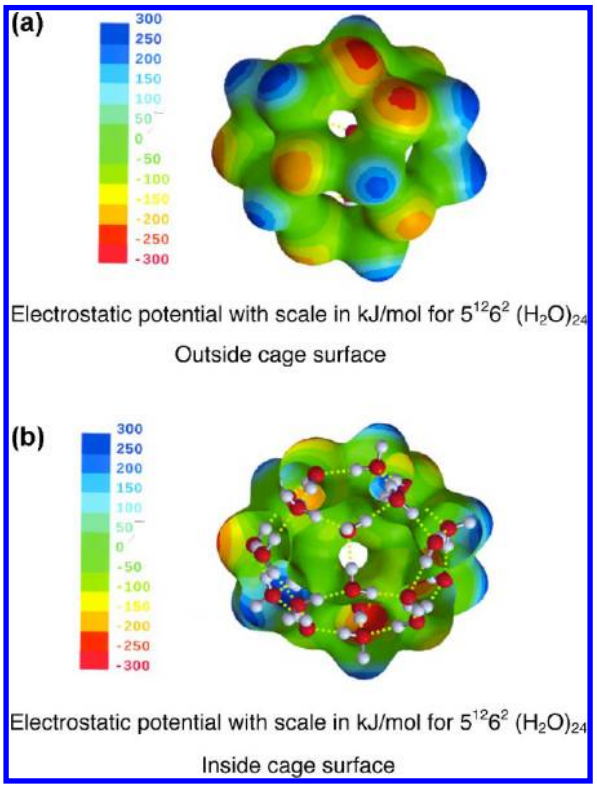

Figure 17. (a) Electrostatic potential with scale in kJ/mol for $5^{12}6^2$ $(H_2O)_{24}$, outside cage surface. (b) Electrostatic potential with scale in kJ/mol for $5^{12}6^2$ $(H_2O)_{24}$, inside cage surface.

cage are, as expected, quite electrostatically positive whereas the surface oxygens are quite electrostatically negative. We were surprised that the potential inside the cage is relatively uniform and quite small. Without showing the explicit atom positions, it would be difficult to locate the hydrogen atoms on the basis of the potential map. The electrostatic potential inside the cage only varies from +28 to −80 kJ/mol. We examined the internal electrostatic potential for connected cages and found that they are also relatively small compared to the outside of the cages. We have also tested whether guests inside the cage result in more polarization of the cage, and found no significant effects. We have not found any discussion of the low electrostatic potential inside of clathrate cages in the literature, and we believe that this will be a fruitful topic for future work. This work suggests that van der Waals forces dominate the guest−host interaction energy, with electrostatic forces playing a smaller role. More sophisticated calculations than those presented here would be required to confirm this conclusion from our work.

CONCLUSION

We have demonstrated that by molecular mechanics simulation of the guest position inside a hydrate cage with fixed water molecules yields useful insight for the prediction of clathrate type and the guest orientation within the cages. Forty-six of forty-seven clathrate types are successfully predicted by this model, and the one case in disagreement with the model the prediction is ambiguous. We also can find the calculated positions and orientation of guest molecules in cages that are consistent with diffraction data and yield new insight that is obscured by the complexity of the diffraction data analysis. In the cases for which several minima for the guest molecules are not too different in energy, the calculations yield insight into the temperature dependence of the diffraction data. We also have a method that easily predicts multiple occupation for any guest (except hydrogen), as well as the geometry for various multiple occupations. The results presented here show that the MMFF potential functions are useful for simulating cage/guest interaction energies that are more sophisticated than just including the effective diameter and well depth of the guest−host interaction. The applicability of the MMFF function is perhaps not too surprising given that it was primarily developed to simulate guest−host interactions in aqueous solution. Finally, we present a density functional calculation of the electrostatic potential inside and outside of the cages. We were surprised to learn how neutral the potential is inside the cage, and we have not seen a discussion of this point in the literature. This result suggests that van der Waals forces will dominate the determination of the guest/host cage energy and orientation.

ASSOCIATED CONTENT

Supporting Information

Coordinates of the cages, all the energy calculations for each guest/cage and for the various types of clathrates, and figures of the cages in both stick and atom representations as well as the Spartan MMFF94 Compliance Statement. This information is available free of charge via the Internet at http://pubs.acs.org.

AUTHOR INFORMATION

Corresponding Author

*E-mail: ebfleisc@chem.ps.uci.edu. Phone: (949) 824-3820.

Notes

The authors declare no competing financial interest.

†E-mail: kcjanda@uci.edu. Phone: (949) 824-5266.

ACKNOWLEDGMENTS

We thank Filipp Furche, Warren Hehre, and Douglas Tobias for useful discussions during the formulation, implementation, and interpretation of our calculations. Their interest and advice was very helpful. We thank the referees for their very careful and critical reading of our manuscript and making suggestions for changes that greatly improved the paper. This work was supported by the National Science Foundation Grant CHE-0404743 and CHE-0911686, the UCI Physcial Sciences Committee on Research, and the EBF Foundation.

REFERENCES

(1) Sloan, E. D.; Koh, C. A. *Clathrate Hydrates of Natural Gases*, 3rd ed.; CRC Press: Boca Raton, FL, 2007.
(2) *Spartan'10*; Wavefunction, Inc.: Irvine, CA, 2010.
(3) *Crystal Maker*; Crystal Maker Software Limited: Sandy Lane, Yarnton, 0X5 1PF, United Kingdom.
(4) Kirov, M. V. *J. Struct. Chem.* **2002**, *43* (5), 790−797.
(5) Anick, D. J. *J. Mol. Struct.* **2002**, *587*, 97−110, 87−96.
(6) Kirov, M. V.; Fanourgakis, G. S.; Xantheas, S. S. *Chem. Phys. Lett.* **2008**, *461*, 180−188.
(7) Yoo, S.; Kirov, M. V.; Xantheas, S. S. *J. Am. Chem. Soc.* **2009**, *131*, 7564−7566.
(8) McDonald, S.; Ojamäe, L.; Singer, S. J. *J. Phys. Chem. A* **1998**, *102*, 2824−2832.
(9) Kuo, J.; Coe, J. V.; Singer, S. J.; Band, Y. B.; Ojamäe, L. *J. Chem. Phys.* **2001**, *114* (6), 2527−2540.
(10) Tanaka, H.; Kiyohara, K. *J. Chem. Phys.* **1993**, *98* (10), 8110−8118.
(11) Kuo, J.; Ciobana, C. V.; Ojamäe, L.; Shavitt, I.; Singer, S. J. *J. Chem. Phys.* **2003**, *118* (8), 3583−3588.

(12) Ludwig, R.; Appelhagen, A. *Angew. Chem., Int. Ed.* **2005**, *44*, 811−815.
(13) (a) Hori, A.; Hondoh, T. *Can J. Phys.* **2003**, *81*, 33−38. (b) Li, Q.; Kolb, B.; Roman-Perez, G.; et al. *Phys. Rev. B* **2011**, *84*, 153103-1−4. (c) Lenz, A.; Ojamäe, L. J. *Phys. Chem* **2011**, *115*, 6169−6176.
(14) Kumar, P.; Sathyamurthy, N. *J. Phys. Chem. A* **2011**, *115*, 14276−14281.
(15) Khan, A. *J. Mol. Struct. (THEOCHEM)* **2003**, *664*−*665*, 237−245.
(16) Schofield, D. P.; Jordan, K. D. *J. Phys. Chem. A* **2009**, *113*, 7431−7438.
(17) (a) Cao, Z.; Tester, J. W.; Trout, B. L. *J. Chem. Phys.* **2001**, *115*, 2550−2559. (b) Anderson, B. J.; Tester, J. W.; Trout, B. L. *J. Phys. Chem. B* **2004**, *108*, 18705−18715.
(18) (a) Halgren, H. A. *J. Comput. Chem.* **1996**, *17* (5−6), 490−519, 520−552, 553−586, 616−641. (b) Halgren, H. A.; Nachbar, R. B. *J. Comput. Chem.* **1996**, *17* (5−6), 587−641.
(19) Kirchner, M. T.; Boese, R.; Billups, W. E.; Norman, L. R. *J. Am. Chem. Soc.* **2004**, *126*, 9407−9412.
(20) (a) van der Waals, J. H.; Platteeuw, J. C. *Nature* **1959**, *183* (4659), 462. (b) van der Waals, J. H.; Platteeuw, J. C. *Adv. Chem. Phys.* **1959**, *2*, 1−57.
(21) (a) McMullan, R. K.; Kvick, A. *Acta Crystallogr.* **1990**, *B46*, 390−399. (b) McMullan, R. K.; Jeffrey, G. A. *J. Chem. Phys.* **1965**, *42* (8), 2725−2732.
(22) Hollander, F.; Jeffrey, G. A. *J. Chem. Phys.* **1977**, *66* (10), 4699−4706.
(23) Udachin, K. A.; Enright, G. D.; Ratcliffe, C. I.; Ripmeester, J. A. *J. Am. Chem. Soc.* **1997**, *119*, 11481−11486.
(24) Rondinone, A. J.; Chakoumakos, B. C.; Rawn, C. J.; Ishii, Y. *J. Phys. Chem B* **2003**, *107*, 6046−6050.
(25) Udachin, K. A.; Ratcliffe, C. I.; Ripmeester, J. A. *J. Phys. Chem. B* **2001**, *105*, 4200−4204.
(26) Udachin, K. A.; Ratcliffe, C. I.; Ripmeester, J. A. *J. Phys. Chem. B* **2007**, *111*, 11366−11372.
(27) Takeya, S.; Udachin, K. A.; Moudrakovski, I. L.; Susilo, R.; Ripmeester, J. A. *J. Am. Chem. Soc.* **2010**, *132*, 524−531.
(28) Lokshin, K. A.; Zhao, Y.; He, D.; Mao, W. L.; Mao, H. K.; Hemley, R. J.; Lobanov, M. V.; Greenblatt, M. *Phys. Rev. Lett.* **2004**, *93* (12), 125503-1−4.
(29) Roman-Perez, G.; Moaied, M.; Soler, J. M.; Yndurain, F. *Phys. Rev. Lett.* **2010**, *105* (14), 145901(4).
(30) Itoh, H.; Tse, J. S.; Kawamura, K. *J. Chem. Phys.* **2001**, *115* (20), 9414−9420.
(31) Manakov, A. Y.; Voronin, V. I.; Kurnosov, A. V.; Teplykh, A. E.; Komarov, V. Y.; Dyadin, Y. A. *J. Inclusion Phenom. Macrocyclic Chem.* **2004**, *48*, 11−18.
(32) Mao, W. L.; Mao, H.; Goncharov, A. F.; Struzhkin, V. V.; Guo, Q.; Hu, J.; Shu, J.; Hemley, R. J.; Somayazulu, M.; Zhao, Y. *Science* **2002**, *297*, 2247−2249.
(33) Alavi, S.; Ripmeester, J. A.; Klug, D. D. *J. Chem. Phys.* **2006**, *125*, 104501-1−10.
(34) Srivastava, H. K.; Sastry, G. N. *J. Chem. Phys. A* **2011**, *115*, 7633−7637.
(35) Struzhkin, V. V.; Militzer, B.; Mao, W. L.; Mao, H.; Hemley, R. J. *Chem. Rev.* **2007**, *107*, 4133−4151.
(36) Patchkovskii, S.; Tse, J. S. *Proc. Natl. Acad. Sci. U. S. A.* **2003**, *100* (25), 14645−14650.
(37) Chou, I.; Sharma, A.; Burruss, R. C.; Shu, J.; Mao, H.; Hemley, R. J.; Goncharov, A. F.; Stern, L. A.; Kirby, S. H. *Proc. Natl. Acad. Sci. U. S. A.* **2000**, *97* (25), 13484−13487.
(38) Martin, A. *J. Phys. Chem. B* **2010**, *114*, 9602−9607.